

Soft Matter

Accepted Manuscript



This is an *Accepted Manuscript*, which has been through the Royal Society of Chemistry peer review process and has been accepted for publication.

Accepted Manuscripts are published online shortly after acceptance, before technical editing, formatting and proof reading. Using this free service, authors can make their results available to the community, in citable form, before we publish the edited article. We will replace this *Accepted Manuscript* with the edited and formatted *Advance Article* as soon as it is available.

You can find more information about *Accepted Manuscripts* in the [Information for Authors](#).

Please note that technical editing may introduce minor changes to the text and/or graphics, which may alter content. The journal's standard [Terms & Conditions](#) and the [Ethical guidelines](#) still apply. In no event shall the Royal Society of Chemistry be held responsible for any errors or omissions in this *Accepted Manuscript* or any consequences arising from the use of any information it contains.

van der Waals free energy model for solubilization of oil in micelles

Americo Boza Troncoso, Edgar Acosta*

*Chemical Engineering and Applied Chemistry, University of Toronto, 200 College Street, Room 131, Toronto, Ontario M5S3E5

Keywords: molecular interactions, phase behavior, microemulsions, surfactant, oil, water, van der Waals, solubilization, micelles

Abstract

This work introduces the first of a two part thermodynamic framework to estimate the solubilization of nonpolar oils in micelles conformed by nonionic surfactants with linear alkyl tails, considering their configuration and the molecular properties of the constituents. This first part introduces a formal approach to account for the lipophilic (van der Waals) contributions to the free energy of solubilization in spherical micelles. To this end, this work uses two recently developed integration methods for sphere-shell and cone-shell VDW interactions that allow the calculation of surfactant-oil and surfactant-surfactant interactions that take place within the micelles of the solubilization process studied here. The method consists in calculating the free energy of transferring a normal alkane from its continuum, and surfactants monomers from empty micelles to produce an oil swollen micelle. The lipophilic interactions are estimated using the microscopic approach of Hamaker with Lifshitz-based Hamaker constants. The influence of n-alkane and surfactant tail length on the solubilization capacity predicted by the van der Waals free energy model (VDW-FEM) are consistent with experimental trends and it is also consistent with the lipophilic terms included in the semi-empirical Hydrophilic-lipophilic-Difference+Net-Average-Curvature's (HLD-NAC) equation that predicts the phase behavior of microemulsions. As a result, these lipophilic terms can now be defined in terms of molecular interactions and molecular properties.

1 Introduction

Microemulsions are thermodynamically stable mixtures of oil and water stabilized by surfactants and cosurfactants. When the oil solubilizes in a micellar aqueous continuous phase, they form oil in water (type I) microemulsions. Oil in water microemulsions are typically used as drug delivery systems, fragrance delivery systems, cleaning formulations, as part of drilling fluid formulations and others.¹⁻³ One common problem to all these applications is to decide what is the best surfactant to maximize the solubilization of a given oil. Although there are practical guidelines, it is desirable to systematically engineer surfactant-oil-water systems using molecular thermodynamic models that could be simple enough to be solved using personal computers, and that use simple set of molecular properties. This work is an effort to contribute towards such an objective.

Simulating the formation of self aggregating systems, such as microemulsions, is a complex subject because these structures change their configuration depending on the surfactant/oil structure, the solution conditions and compositions. It has been proposed that simulating these systems requires performing a balance of lipophilic and hydrophilic energetic contributions to their total energy of formation.^{4,5} Some of these contributions were conceived conceptually or estimated through phenomenological models that incorporated molecular configurations and some form of molecular interactions.⁶⁻¹¹ Most of the phenomenological approaches emphasized the inter-aggregate interactions over the intramicellar energetic contributions to the total free energy of the aggregate formation. More recent efforts also considered intra-micellar contributions, indirectly, via the analysis of the bending energy of the droplet at the interface.^{8,11,12} Mitchell and Ninham, and Nagarajan and Ruckenstein proposed models to simulate micelle or microemulsion formation with emphasis in intramicellar considerations assuming no interactions between aggregates at low aggregate concentrations.^{10,13} However, they did not elaborate on the critical role that the oil could have driving the existence of microemulsions or their phase behavior. All these previous efforts introduced important concepts such as the packing of surfactants, oil and water in micelles and reverse micelles, and the various interactions that are relevant to the solubilization process. Other modeling approaches, such as molecular dynamics and Monte Carlo simulations have also been used to predict the phase behavior of simplified systems.¹⁴⁻¹⁸

The lipophilic interactions have been proposed as one of the most important contributions driving the process of self assembly.^{5,19-24} For example, increasing the surfactant tail length usually results in increased solubilization capacity of hydrocarbons in micelles.^{1,2,25} Also, for a micelle conformed by a given surfactant, the amount of alkane solubilized in micelles has been observed to decrease with increasing size of the alkane.^{1,26-28} To account for the different oil solubilization features and solubilization peculiarities observed in practice,²⁷ it is necessary to develop a formal framework to account for the lipophilic contributions to microemulsion formation. An original approach to incorporate interactions to understand the thermodynamics of microemulsions was introduced by Winsor with the so called R_w ratio of the surfactant interactions with oil and water, as:²⁹

$$R_w = \frac{A_{CO}}{A_{CW}} \quad (1)$$

The subscripts CO and CW stand for the surfactant-oil and surfactant-water interactions, respectively. Later, an expanded version was proposed.^{28,30}

$$R_w = \frac{A_{CO} - A_{OO} - A_{LL}}{A_{CW} - A_{WW} - A_{HH}} \quad (2)$$

where the subscripts OO and WW represent the self-interactions of oil and water molecules, respectively. LL and HH are the self-interactions of the surfactant's lipophilic and hydrophilic moieties, respectively. Winsor understood the phase behavior of microemulsions as a ratio of hydrophilic and lipophilic interactions and even though the framework considered the contribution of the molecular interactions, no one has been able to calculate those interactions thus far. In the form of a free energy model, Equation 2 should be expressed as a balance of the interactions, rather than their ratio.⁴ It is important here to emphasize that the Winsor's expanded equation already accounts for six interactions, which as explained later, are in part at the heart of the VDW-FEM. It is known that the curvature of micelles determine the amount of oil that can be solubilized in a micelle.^{2,31} Ninham and Lo Nostro refer that the curvature is set predominantly by molecular interactions.¹⁹ Israeachvili et al. suggested that the geometry and the interactions, within self-aggregated systems, should be considered to construct a formal model to simulate the behavior of microemulsions.⁹ In agreement to this approach, Chung Hu introduced a model based on the integration of VDW interactions in a lamellar-type configuration to estimate the interfacial

tension and the solubilization of oil and brine in middle phase microemulsions.³² Nagarajan and Ruckenstein also introduced a model based on molecular interactions and a spherical configuration of oil-swollen micelles aggregates to predict the phase behavior of microemulsions.¹³ Even though the Nagarajan-Ruckenstein model uses only molecular properties, the surfactant-oil interactions were considered through solubility parameters, making it difficult to account properly for the oil's role in forming microemulsions. One of the limitations in calculating the intramicelle interactions in spherical configurations is that there were no expressions for the VDW interactions between a spherical core (the oil core of a swollen micelle) and the surfactant tail shell. We recently introduced and validated VDW integration methods for cone-shell and sphere-shell configurations necessary for the calculation of these intramicelle interactions.³³ Using these recent integration methods is now possible to calculate the free energy associated with the extraction of oil from its continuous phase and surfactant monomers from micelles to produce a new oil-swollen micelle. It is also possible to calculate the surfactant-surfactant and surfactant-oil interactions in the new oil-swollen micelle. The VDW-FEM assumes that the aggregates are diluted enough to neglect intermicellar interactions. Additionally, the VDW-FEM is able to reflect, from molecular properties, the solubilization features of nonpolar oils in micelles with variation of the surfactant tail size and type of alkane in agreement to experimental observations.^{1,26}

At this point, the VDW-FEM does not account for the role of the hydrophilic energetic contributions to the solubilization process. Some of these contributions favor the solubilization process while others oppose it. It will be shown in an upcoming publication the inclusion of these contributions into the VDW-FEM does not alter the solubilization trends presented here as a result of the interplay of surfactant tails and nonpolar oils. The hydrophilic energetic contributions to solubilization are estimated from the conformational changes in the micelle's hydrophilic shell layer when the oil solubilizes in the lipophilic interior of the micelle.

To further test/validate the VDW-FEM model, the predictions of solubilization capacity with different alkanes was compared to the experimental trends obtained from the Hydrophilic-Lipophilic-Difference (HLD) and the net average curvature framework (NAC) framework. The HLD-NAC is a semi-empirical model used to predict solubilization phase transitions, phase volumes, microemulsion morphology,

microemulsion viscosity and interfacial tension of real systems. Due to their success in practice, the HLD-NAC framework has been used as benchmark to compare the performance of recent thermodynamic models for microemulsions.^{34,35} Despite the capabilities of the HLD-NAC, its semi-empirical origin does not offer a deeper understanding on the connection between phase behavior and molecular interactions. This disconnection prevents the extrapolation of the HLD-NAC framework to non-conventional systems such as microemulsions involving supercritical fluids, ionic liquids, and non-aqueous hydrophilic phases.^{36,37} Overcoming this limitation is part of the aim of this work. To this end, we compared the HLD-NAC predicted effect of the size of the n-alkane on its solubilization capacity with the effect predicted by the VDW-FEM. It was found that the VDW-FEM not only confirms the experimental trends represented in the HLD-NAC, but also predicts the K value of the HLD equation. Additional details on the HLD and NAC equations are found in the Appendix C.

2 Model Development

To model the solubilization of oils in micelles, it is assumed that oil is taken from its continuum liquid phase to be placed in the core of a micelle and in between the tails of the surfactant. The model is circumscribed to dilute micellar concentrations so that inter-aggregate interactions are neglected. It is also assumed that surfactants are taken up from empty micelles and placed in oil-swollen micelles, as depicted in Figure 1. This scheme is inspired in the solubilization mechanism proposed by Carrol and in free energy calculation methods used by other authors to estimate the Gibbs free energy of self-association.^{5,38}

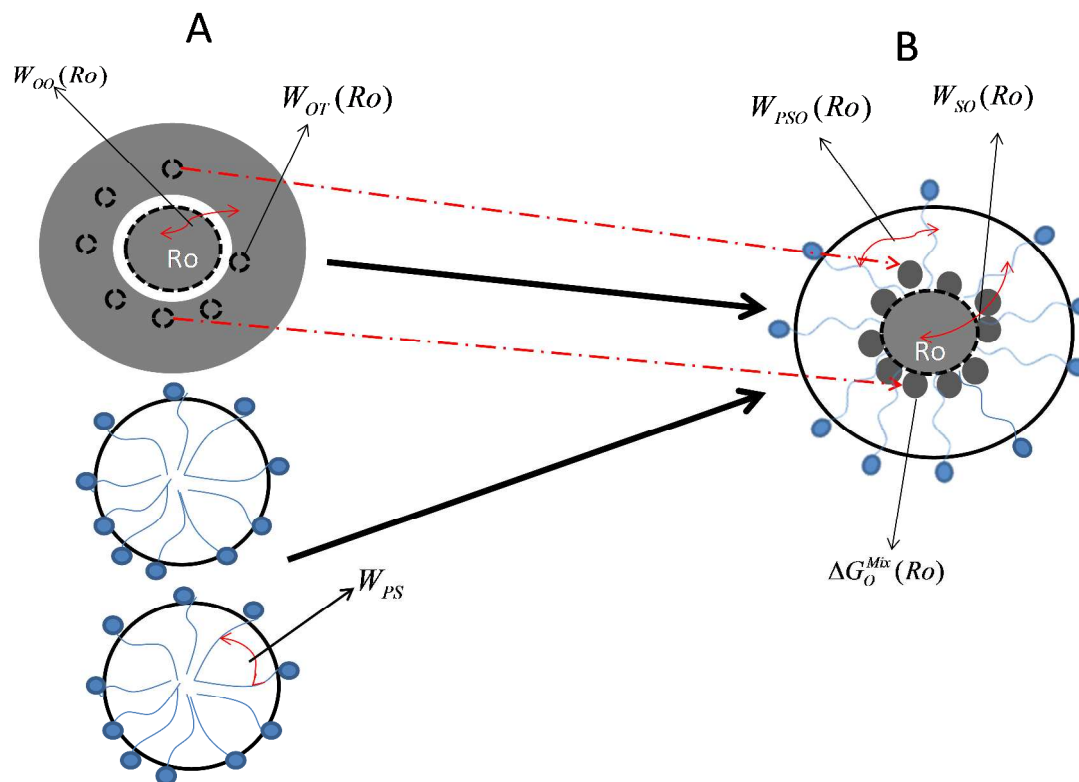


Figure 1. Schematic representation of solubilization of oil in micelles. A: Initial State: Oil in oil-continuous media and empty micelles in aqueous continuous media. B: The micelle takes up an oil drop with a radius R_o and individual oil molecules are taken to be solubilized in the tail domain of the micelle. $W_{oo}(R_o)$ and $W_{so}(R_o)$ represent the oil-oil and surfactant-oil interactions. $W_{or}(R_o)$ reflects the energy needed to extract the individual oil molecules from the oil. W_{ps} and $W_{ps_o}(R_o)$ identify the surfactant-surfactant interactions in empty and swollen micelles, respectively. $\Delta G_o^{Mix}(R_o)$ represents the energy of mixing oil molecules in between surfactant tails. R_o is the oil droplet radius in the core.

In this framework, the solubilization capacity of oils in micelles is determined computing the total free energy of solubilization of oil in the core and in the surfactant tail domain of a swollen micelle. This total free energy change can also be understood as the reversible work associated with oil solubilization in micelles at constant temperature and pressure:

$$W_T(R_o) = W_{so}(R_o) - W_{oo}(R_o) - W_{or}(R_o) + W_{ss}(R_o) + \Delta G_o^{Mix}(R_o) \quad (3)$$

Equation 3, at this point, contains the key lipophilic interactions proposed by Winsor in the “R” ratio or its modifications, but lacks terms associated with changes in hydrophilic interactions. In a subsequent publication, Equation 3 will include these hydrophilic contributions. The energetic contributions that favor the oil solubilization process estimated through Equation 3 are identified with positive signs while the unfavorable contributions take negative signs implying energy required or costs. Thus, $W_{so}(R_o)$

represents the surfactant tail-oil interaction in the swollen micelle. $W_{OO}(Ro)$ reflects the oil-oil interaction and represents the energy cost associated with extracting the oil core from its liquid phase. $W_{OT}(Ro)$ represents the energy required to extract oil molecules from its continuum phase to be solubilized in between the surfactant tails. $W_{SS}(Ro)$ represents the net free energy change in surfactant-surfactant tail interactions in the empty micelle (W_{PS}), and in the oil-swollen micelle ($W_{PSO}(Ro)$). In addition to these interactions, a contribution of mixing $\Delta G_O^{Mix}(Ro)$ surfactant tails with the oil in the surfactant tail domain is also considered. Descriptions of these contributions and the equations used to calculate them are presented in the following sections and the appendices.

The first four terms of Equation 3 can be calculated by integrating the VDW interactions between bodies of known geometries, using the microscopic approach of Hamaker.^{31,39} This method consists in obtaining, first, the interaction of a hard sphere molecule with a particle of interest (spherical, cylindrical, etc) via integration and then integrating again the expression to obtain the interaction between the two macroscopic bodies. This integration method has been described by Israelachvili in ample details.³¹ The general expression to obtain such interparticle interactions is:⁴⁰

$$W(r) = \int \int_{V_2 V_1} \frac{-C \rho_1 \rho_2 dV_1 dV_2}{r^6} \quad (4)$$

where ρ_1 , and ρ_2 are the molecular densities of the interacting bodies and V_1 and V_2 their volumes, respectively; r is the separation distance between molecules and C is the VDW dispersion coefficient, which is given by:³¹

$$C = \frac{3\alpha_{PA}\alpha_{PB}I_A I_B}{(4\pi\epsilon_0)^2(I_A + I_B)} \quad (5)$$

where α_{PA} and α_{PB} are the molecular polarizabilities of the interacting molecules. I_A and I_B are their first ionization potentials. ϵ_0 is the vacuum permittivity. The VDW interaction potentials between different bodies can be obtained using Equation 4 and they are expressed in terms of the Hamaker constant:³¹

$$A = \pi^2 C \rho_1 \rho_2 \quad (6)$$

Equation 6 assumed pairwise additive interactions, which is suitable for less dense materials. For dense materials, multiple interactions can influence the net interaction between bodies. One approach to consider these multiple interactions is the use of a modified Hamaker constant calculated considering the electrodynamic properties of the materials, via a continuum approach based on the Lifshitz theory. This approach is preferred for dense condensed systems where multiple interactions can distort the additivity assumption of the interactions. The nonretarded Lifshitz-based Hamaker constant for bodies 1 and 2 interacting across a medium 3 is:³¹

$$A_{ls}(T) = \frac{3}{4} kT \left(\frac{\varepsilon_1 - \varepsilon_3}{\varepsilon_1 + \varepsilon_3} \right) \left(\frac{\varepsilon_2 - \varepsilon_3}{\varepsilon_2 + \varepsilon_3} \right) + \frac{3h\nu_e}{8\sqrt{2}} \frac{(n_1^2 - n_3^2)(n_2^2 - n_3^2)}{(n_1^2 + n_3^2)^{0.5}(n_2^2 + n_3^2)^{0.5}\{(n_1^2 + n_3^2)^{0.5} + (n_2^2 + n_3^2)^{0.5}\}} \quad (7)$$

In this equation, T is the absolute temperature, k the Boltzmann constant, ε the dielectric constant, h the Planck's constant, ν_e the characteristic absorption frequency and n the refractive index. When bodies 1 and 2 are identical, Equation 7 reduces to:³¹

$$A_{ls-i}(T) = \frac{3}{4} kT \left(\frac{\varepsilon_1 - \varepsilon_3}{\varepsilon_1 + \varepsilon_3} \right)^2 + \frac{3h\nu_e}{16\sqrt{2}} \frac{(n_1^2 - n_3^2)^2}{(n_1^2 + n_3^2)^{3/2}} \quad (8)$$

ε_3 and n_3 take a value of 1 when the intervening medium is vacuum or air. In this work, it is assumed that the intervening medium is vacuum. The dielectric constant of liquids can be calculated using the following correlation:⁴¹

$$\varepsilon_i(T) = a + b * T + c * T^2 + d * T^3 \quad (9)$$

where a , b , c and d are coefficients that fit the dielectric constant's value with temperature. The refractive index can be simply calculated by the following Maxwell relation:⁴²

$$n_i = \sqrt{\varepsilon_i} \quad (10)$$

The integration of the VDW interactions in the VDW-FEM requires the use of the sphere-shell and cone-shell geometrical configurations developed and validated in our previous work.³³ Both expressions apply to spherical configurations. For VDW-FEM, Lifshitz-based Hamaker constants are used due to the fact that this combination produces better predictions of alkane's surface tension.³³ Retardation effects are ignored due to the very small separation distances considered (less than 10nm).³³

2.1 Surfactant-oil $W_{SO}(Ro)$ Interaction.

To calculate the surfactant-oil interaction, a sphere-shell configuration is used, as depicted in Figure 2A. The spherical shell represents the surfactant tail domain and the inner sphere the oil solubilized in the core. The estimation of the surfactant-oil $W_{SO}(Ro)$ interaction proceeds using the non-retarded sphere-shell interaction potential:³³

$$W_{SO}(Ro) = \frac{-16Ro^3 A_{SO}}{3} \int_{Ro+\delta}^{Ro+\delta+L_s} \frac{\zeta^2 d\zeta}{(\zeta^2 - Ro^2)^3} \quad (11)$$

where Ro is the radius of oil solubilized in the core of a micelle and L_s is the surfactant tail length. δ is an interfacial separation distance, defined in the literature to be 0.165nm.³¹ In this case, it establishes the separation distance between the oil drop and the tail domain. A_{SO} is the surfactant-oil Hamaker constant computed on the basis of the Lifshitz theory using Equation 7. It is important to note that swollen micelles not only contain surfactant tails in their tail domain but also oil occluded in between them, as discussed in subsequent sections. Hence, the shell of Figure 2A should be understood to contain surfactant tails and oil in between them. However, the integration method used to estimate the surfactant-oil interactions as

well as the method employed to estimate the Hamaker constant lie on within-body uniform density assumptions. To meet this requirement, it is assumed that the tail domain of a swollen micelle, containing surfactant tails and oil, has the electrostatics properties equivalent to that of a closely-packed shell composed of surfactant tails only. This approximation is necessary in order to solve the two-body problem of Equation 11. The largest deviation in Lifshitz-based Hamaker constant for the alkanes considered in this work (from hexane to hexadecane) is close to 20%.³³ However, as discussed later, the volume fraction of the occluded oil in the tail domain is typically 30% or less, meaning that the approximate error associated with this simplification is 6% or less.

2.2 Energy cost of extracting core oil from continuous oil phase $W_{oo}(Ro)$

The oil-oil interaction $W_{oo}(Ro)$ represents the free energy cost of extracting an oil drop (that will be placed in the core of the swollen micelle) from its continuum oil phase. The continuum oil phase can be considered to be a shell that encloses a spherical oil drop. This interaction can be calculated using again the VDW integration applied to a sphere-shell configuration:³³

$$W_{oo}(Ro) = \frac{-16Ro^3 A_{oo}}{3} \int_{Ro+\delta}^{Ro+\delta+\Omega} \frac{\zeta^2 d\zeta}{(\zeta^2 - Ro^2)^3} \quad (12)$$

where A_{oo} is the Lifshitz-based oil-oil Hamaker constant that can be calculated using Equation 8. It has been determined that as long as the shell thickness Ω is about 2.3 nm or larger it represents the interaction with the bulk oil phase.³³ This inter-particle interaction is illustrated in Figure 2B.

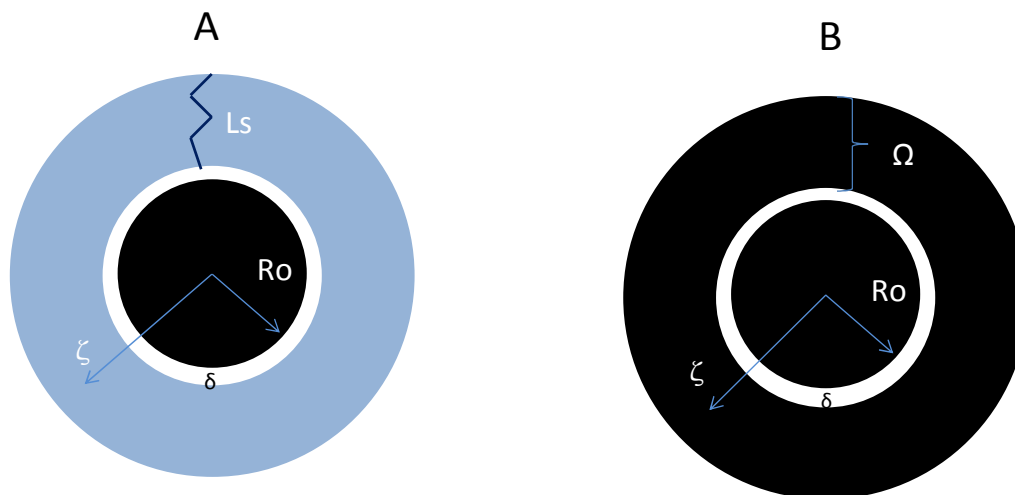


Figure 2. Cross-sectional views of spheres within spherical shells. A: Represents an oil drop enclosed by surfactant tails with a length of L_s . δ is an interfacial separation distance and ζ a vector that goes from the center of the inner sphere to the outer diameter of the spherical shell. B: Represents an oil drop surrounded by its liquid phase. Ω is a shell length representing the continuum that encloses the drop.

2.3 Pure surfactant tail interactions $W_{SS}(Ro)$

To calculate the free energy change associated with the formation of an oil swollen micelle from an empty micelle, it is necessary to estimate the surfactant-surfactant interactions when the micelle is empty W_{PS} and when the micelle is swollen $W_{PSO}(Ro)$. W_{PS} account for interactions between the tail of a surfactant tail and the rest of tails in an empty micelle. $W_{PSO}(Ro)$ accounts for the interaction of a surfactant tail with tails and oil molecules in the tail domain of a swollen micelle, as schematically represented in in Figures 3A and 3B. The net interaction $W_{SS}(Ro)$ is calculated as:

$$W_{SS}(Ro) = N_{AT}(Ro)W_{PSO}(Ro) - N_{AR}(Ro)W_{PS} \quad (13)$$

where $N_{AT}(Ro)$ stands for the aggregation number of surfactant tail equivalents in the tail domain. $N_{AT}(Ro)$ includes the real surfactant aggregation number $N_{AR}(Ro)$, and an additional number of surfactant tail equivalents that would account for the volume of oil solubilized in the tail domain. In undertaking this

approximation, it is assumed that the electrodynamic properties of the solubilized oil are similar to that of the tail of the surfactant, as discussed in section 3.1. The procedure to estimate both aggregation numbers is described in the Appendix A. Equation 13 can be interpreted as the free energy of transferring surfactant tails $N_{AR}(Ro)$ from empty micelles to swollen micelles. It also contains the energetic contribution of the surfactant-oil interactions in the tail domain of swollen micelles.

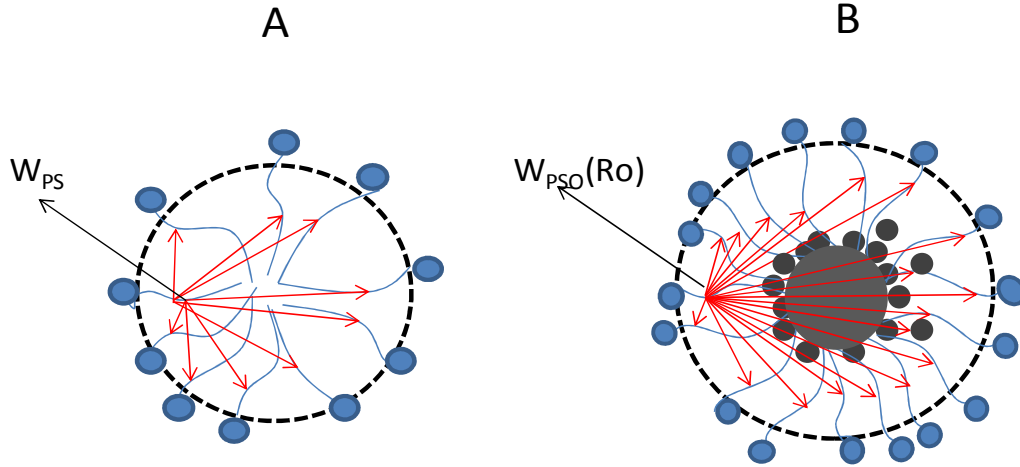


Figure 3. A: The red arrows represent the interaction of a surfactant tail with the rest of tails of an empty micelle. B: The arrows represent the interaction of a tail with the rest of tails and oil molecules solubilized in the tail domain.

The VDW interactions of a surfactant tail with the tail domain of an empty or a swollen micelle can be integrated considering the interaction of a truncated cone with a coneless shell, depicted in Figure 4. For an empty micelle, the integration of the VDW interaction yields:³³

$$W_{PS} = - \int_{d_o}^{d_o+0.8L_s} \int_{d_o}^{d_o+0.8L_s} \int_{\alpha_2}^{\pi} \frac{4A_{SS}y^2 x^2 \sin \alpha \left[\frac{1}{(\cos(\alpha_1))^3} - \frac{1}{(\cos(\alpha_1))^2} \right]}{[x^2 + y^2 - 2xy \cos(\alpha)]^3} d\alpha dy dx \quad (14)$$

The upper integration limit of Equation 14 expresses the fact that, according to the literature, the tails only stretch 80% of their extended length (L_s) in empty micelles. **Error! Bookmark not defined.** The lower integration limit considers the same packing restriction of extending all the surfactant tails to the center of the empty micelle, setting an empty volume of radius d_o in the center of the micelle as 20% the

length of the surfactant ($d_o=0.2L_s$). The term A_{SS} is the surfactant-surfactant Hamaker constant, calculated with Equation 8. The angle α_2 sets the initial integration boundary of the coneless shell and α_1 defines the angle of the cone that represents a surfactant tail of an empty micelle. Figure A1 in Appendix A describes the geometry associated with Equation 14. The procedure to estimate these angles is described in Appendix B, and in the original publication that describes the VDW integration in coneless shell configurations.³³

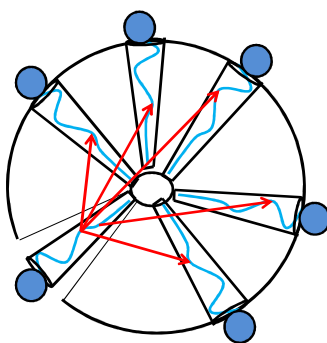


Figure 4. The interaction of a cone with a coneless shell. The cone represents a surfactant tail and the coneless shell the rest of surfactant tails in the same micelle.

The interactions of a surfactant tail with the tail domain of an oil-swollen micelle $W_{PSO}(Ro)$ are illustrated in Figure 3B. To estimate $W_{PSO}(Ro)$, Equation 14 was adapted for oil-swollen micelles:

$$\begin{aligned}
 & W_{PSO}(Ro) \\
 &= - \int_{R_o+\delta}^{R_o+\delta+L_s} \int_{R_o+\delta}^{R_o+\delta+L_s} \int_{\alpha_{2s}(Ro)}^{\pi} \frac{4A_{SS}y^2 x^2 \sin \alpha \left[\frac{1}{(\cos(\alpha_{ms}(Ro)))^3} - \frac{1}{(\cos(\alpha_{ms}(Ro)))^2} \right]}{[x^2 + y^2 - 2xy \cos(\alpha)]^3} d\alpha dy dx \quad (15)
 \end{aligned}$$

The oil solubilized in the core is considered by introducing the core drop radius, Ro , in the lower limit of integration in the radial direction. In addition, an interfacial separation distance δ between the core

oil and the tail domain is considered. The angles $\alpha_{2s}(Ro)$ and $\alpha_{ms}(Ro)$ are the equivalent of α_2 and α_1 , respectively, for oil-swollen micelles, and their calculation is described in Appendix B.

As indicated in section 3.1, to employ the Lifshitz continuum approach to calculate the Hamaker constant (A_{ss}) for Equation 15, we assumed that the electrostatics properties of the surfactant tail domain are those of the surfactant tails. For the case of the n-alkanes studied in this work, this represents a maximum deviation of 6% when the surfactant tail is C_{16} , and C_6 is the solubilized oil.

2.4 Energy required to solubilize oil in the tail domain $W_{OT}(Ro)$.

Experimental evidence demonstrates that oils not only solubilize in the core of micelles but also in between surfactant tails (the tail domain).^{1,43} Therefore, it is necessary to calculate the free energy cost of extracting individual oil molecules, from the oil phase, to be solubilized in the tail domain. Because we are extracting individual oil molecules, and not an oil drop, it is expected that this energy can be represented as a fraction of the cohesive energy of the oil. The magnitude of that fraction would depend on the coordination of the molecule in the oil phase.

To estimate the free energy cost to solubilize oil in the tail domain, we consider an oil molecule lying on top of the oil drop that will be solubilized in the core of the oil-swollen micelle, as shown in Figure 5A. Figure 5A presents this oil molecule in two configurations, a short conformation where the volume of the shell formed between R_o and R_e is equivalent to the volume of oil solubilized in the tail domain, and the second is an extended conformation, equivalent to the extended length of the oil molecule. Figure 5A illustrates the molecular interactions that need to be broken, for the short conformation, in order to extract oil molecules from the continuous oil phase. The solid arrows indicate the interactions with the core oil drop, the dashed line the interactions within the shell, and the dot-dashed lines represent the interaction with the rest of the oil phase.

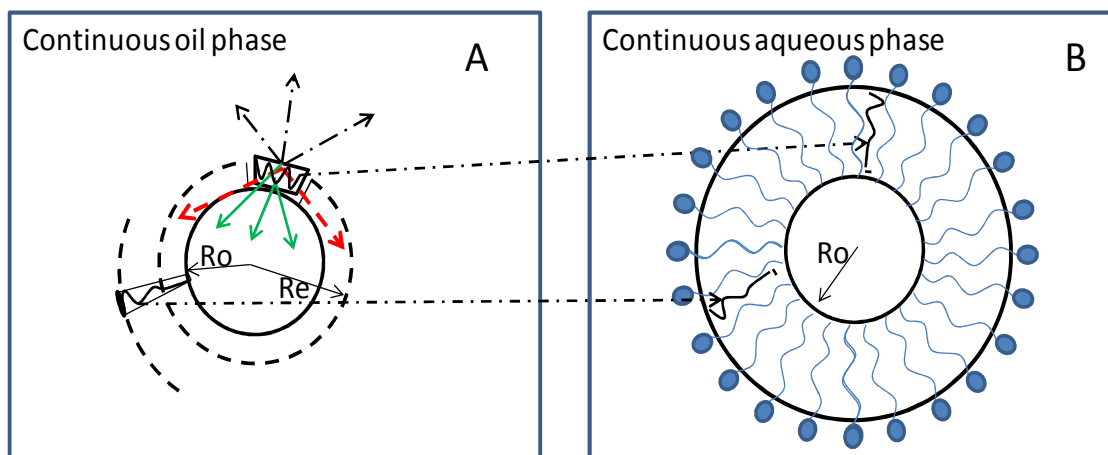


Figure 5. Mechanism of oil solubilization in the tail domain. Part A illustrates the possible short and long conformations of oil molecules that will be solubilized in the tail domain, along with the interactions of the oil molecule within the oil phase. Figure B presents the location of the oil molecules in the tail domain of the swollen micelle.

From all these interactions, the molecule-core interaction has already been considered through Equation 12. The interactions within the shell ($W_{cone-shell}(R_o)$) can be calculated using the core-shell interaction, adapted from Equation 14. The interactions with the rest of the oil can be estimated using a sphere-shell interaction with Equation 12 and dividing by the number of oil molecules in the shell ($W_{bs}(Re(R_o))/N_{OS}(R_o)$), using the exterior radius (Re) appropriate for the conformation of interest. To calculate the fraction ($f(R_o)$) of the cohesive energy (U) required to extract individual molecules of the oil phase, the following expression can be used:

$$f(R_o) = \frac{W_{cone-shell}(R_o) + \frac{W_{bs}(Re(R_o))}{N_{OS}(R_o)}}{U} \quad (16)$$

Figures 6A and 6B show the fraction of the cohesive energy ($f(R_o)$), calculated with Equation 16, as a function of the core radius (R_o) for short and long conformations, respectively, for alkanes solubilized in C_{12} surfactant tails ($N_{cs} = 12$) and headgroup areas (A_s) of 50 \AA^2 at $25 \text{ }^\circ\text{C}$. Figure 6A shows that for the short conformation scenario the asymptotic value of $f(R_o)$ ranges from 0.32 to 0.5, depending on the molecular weight of the alkane. In the long conformation scenario, Figure 6B, the asymptotic value of $f(R_o)$ is close to 0.65 for all the alkanes. For systems with a core radius of 1 nm or less, the full free

energy of cohesion ($f(R_o)=1$) must be used. Calculations of $f(R_o)$ for the extended conformation at 25°C with alternate surfactant tails ($N_{cs} = 10$ and 16) also produced an average value of 0.65. This analysis illustrates that the value of $f(R_o)$ ranges between 0.32 and 0.65. In this work, we refrain from assigning a specific value to $f(R_o)$. The impact of $f(R_o)$ on solubilization free energy, incorporating hydrophilic interactions, will be considered in an upcoming publication. The total energy cost to extract oil to be solubilized in between tails can be estimated as:

$$W_{OT}(R_o) = -I * U * N_{OS}(R_o) \quad (17)$$

Since $f(R_o)$ is approximately constant for core radius larger than 1nm, a constant value “ I ” was used in our calculations. For all the calculations in this work, a value of $I=0.65$ is used to illustrate the magnitudes of the lipophilic terms of the free energy balance (Equation 3).

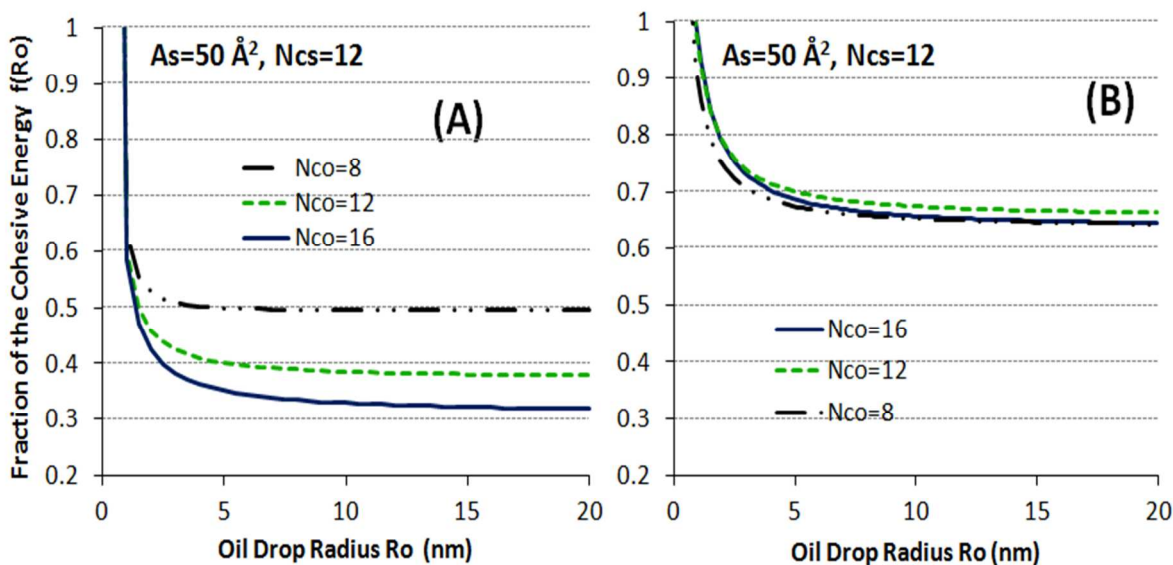


Figure 6. Fraction of the cohesive energy ($f(R_o)$) required to extract molecules from the oil phase to be solubilized in the tail domain for (A) short and (B) long conformations. Calculations carried out using Equation 22 for C_{12} surfactant micelles ($A_s=50 \text{ \AA}^2$) at 25 °C containing solubilized octane ($N_{co}=8$), dodecane ($N_{co}=12$) and hexadecane ($N_{co}=16$).

2.5 Gibbs free energy of mixing $\Delta G_o^{Mix}(Ro)$ oil in between surfactant tails.

The solubilization of oil in the tail domain leads to an intermixing of surfactant tails and oil. The essence of this contribution is entropic, and can be calculated as:³⁹

$$\Delta S_o^{Mix}(Ro) = -\frac{R}{N} * (N_{oS}(Ro) * \ln(x_o(Ro)) + N_{AR}(Ro) * \ln(x_s(Ro))) \quad (18)$$

The approach used to calculate the number of molecules occluded in the surfactant tail domain $N_{oS}(Ro)$ and the surfactant aggregation number $N_{AR}(Ro)$ can be found in the Appendix A. $x_o(Ro)$ and $x_s(Ro)$ are the molecular fraction of oil and surfactant, respectively, in the tail domain. R is the gas constant and N is Avogadro's number. The mixing Gibbs free energy is:³⁹

$$\Delta G_o^{Mix}(Ro) = \Delta H(Ro) - T * \Delta S_o^{Mix}(Ro) \quad (19)$$

where $\Delta H(Ro)$ is the enthalpy of mixing. Considering ideal mixing $\Delta H(Ro) = 0$ due to the similarities between the solubilized alkanes and the alkyl tail groups of the surfactants, and assuming a solubilization processes at constant temperature, Equation 19 is simplified to:

$$\Delta G_o^{Mix} = -T * \Delta S_o^{Mix} \quad (20)$$

This approach considers simple entropy of mixing between the surfactant tails and the oil molecules within the tail domain. There can be additional contributions to this entropy of mixing such as the excess entropy of mixing due to differences in volume of the surfactant tails and the oil molecules, as well as potential solvation phenomena, particularly in the solubilization of polar oils.

3 Results and discussions

To calculate the lipophilic contributions to the free energy of solubilization (Equation 3), the VDW integrals and the related equations described in section 3, and Appendices A and B were implemented in Mathcad ® 15. Although, the set of VDW-FEM equations is simple and does not require iterative

calculations, it still requires the solution of the triple integrals associated with the sphere-shell and the cone-shell configurations. These integrals were numerically solved using the adaptive Romberg method available in Mathcad.

The simulations presented in this work involve the use of five different normal alkanes ranging from hexane ($N_{CO}=6$) to hexadecane ($N_{CO}=16$) and two straight-chain surfactant tails of decyl ($N_{CS}=10$) and dodecyl ($N_{CS}=12$). Hence, the properties of the surfactant tails are assumed to be those of their equivalent alkane molecules such as decane and dodecane. All the estimations in this work were performed at 25 °C and the relevant molecular properties used for estimations are presented in Table 1.

Table 1. Liquid density (ρ), dielectric constant (ϵ), refractive index (η) and cohesive energy (U) of different alkanes used for the calculation of the VDW-FEM lipophilic contributions at 25 °C.

| N_{CO} | ρ_l^a at 25 °C g/cm ³ | ϵ^b | η^c | U^d Cal/mol |
|-----------|------------------------------------------|--------------|----------|------------------|
| 6 | 0.655 | 1.881 | 1.371 | 6982 |
| 8 | 0.698 | 1.94 | 1.393 | 9300 |
| 10 | 0.726 | 1.986 | 1.409 | 11770 |
| 12 | 0.745 | 2 | 1.410 | 14270 |
| 16 | 0.769 ^F | 2.04 | 1.428 | 19300 |

^aNIST webbook.⁴⁴ ^bCalculated with Equation 9. ^cCalculated with Equation 10. ^dMaffiolo et al.⁴⁵ ^FOutcalt et al.⁴⁶

3.1 Oil solubilization and surfactant aggregation based on swollen micelle geometry

There have been some discussions around the solubilization of nonpolar oils in the tail domain of swollen micelles.^{1,27} Several studies indicate that nonpolar alkanes solubilize in the core and in the tail domain.^{43,47}

In the VDW-FEM, the extent to which oil is solubilized in the tail domain is determined by the head group area (A_s), the radius of the core, and the volume of the surfactant tail estimated via Equation A4, following simple geometrical considerations. Although the value of A_s might be influenced by the structure of the hydrophilic head group, this is a value assumed to be constant in this work. This assumption is based on neutron scattering evidence that suggests that the area per molecule of the surfactant remains

approximately constant regardless of the magnitude of the solubilization of oil (associated with core radius, R_o) in micelles.⁴⁸ The relatively small deviations in area per molecule with solubilization radius can be explained by the fact that the contrast matching used in neutron scattering measures the area of the surfactant in contact with either oil or water, but not the exact area at the intersection between the hydrophilic and the lipophilic groups (i.e. the surfactant neck) within the surfactant molecule.⁴⁸

Figure 7 shows the volumes of oil solubilized in the core and in the tail domain of micelles having straight-chain tails of 12 carbons ($N_{CS}=12$) and headgroup areas (A_s) of 50 \AA^2 at $25 \text{ }^\circ\text{C}$ estimated using the VDW-FEM. As observed, the solubilization in the tail domain is larger than in the micellar core at small oil drop radius $R_o \approx 3 \text{ nm}$. After this radius, the solubilization in the core of the micelle is more significant. Molecular dynamic simulation studies, performed by Jönsson et al., have found the same feature for the solubilization of uncharged oils in micelles composed of ionic surfactants.⁴³ Consistent with our simple geometric assumption to represent this solubilization behavior included in the VDW-FEM, Rosen presents also a plausible explanation of the same fact interpreted from experimental observations.¹

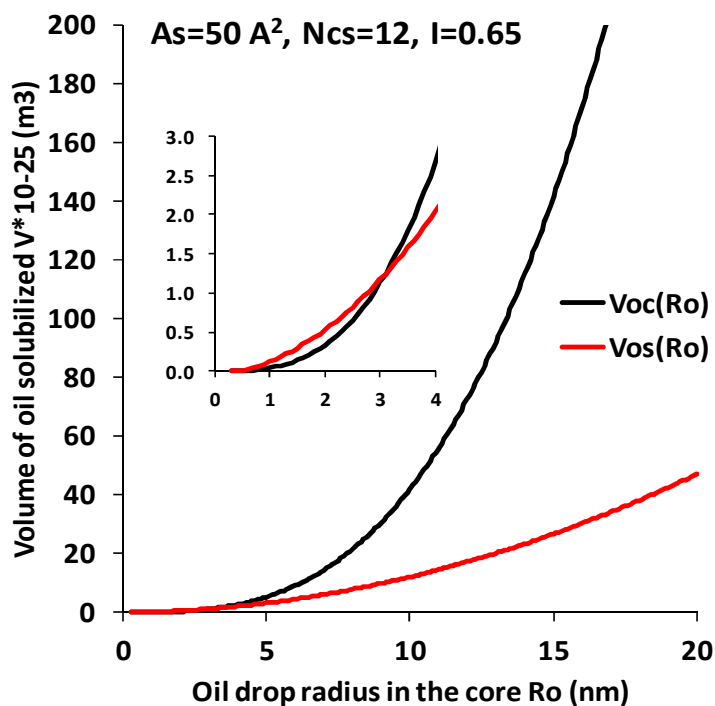


Figure 7. Volume of oil solubilized in the core $V_{oc}(R_o)$ and in the tail domain $V_{os}(R_o)$ of a micelle conformed by single-chain tails of (N_{cs}) 12 carbons and headgroup areas (A_s) of 50 \AA^2 at $25 \text{ }^\circ\text{C}$.

The equations in Appendices A and B also predict that the volume of oil solubilized in the tail domain is approximately 30% of the total volume of the tail domain of the swollen micelle. This volume fraction, strictly speaking, is a function of the core radius and the area of the surfactant (A_s). For the same system of Figure 7, this volume fraction is 18% when the micelle core radius is 1.5 nm, 27% when the core is 2.7 nm, 32% when the core is 4 nm, and 42% when the core is 18 nm.

The surfactant aggregation number in micelles have been extensively studied and reported. However, there are not many studies reporting the aggregation number of surfactants in microemulsions. The calculated values of surfactant aggregation numbers $N_{AR}(R_o)$ obtained using of the VDW-FEM are within the range of some reported values encountered in the literature.^{49,50} In agreement with experimental observations, the VDW-FEM also reflects the fact that the surfactant aggregation number increases with solubilization as well as with increasing surfactant tail chain length.¹ Table 2 presents predicted aggregation numbers for C_{10} , C_{12} and C_{16} surfactant tails at 2, 4, and 6 nm micelle cores.

Table 2. Variation of the aggregation number of hypothetical surfactants having headgroup areas of 50 \AA^2 and different surfactant tails (Ncs) with variations of the amount of oil solubilized in the core at $25 \text{ }^\circ\text{C}$.

| Ro (nm) | $N_{AR}(R_o)$ | | |
|---------|---------------|---------|---------|
| | Ncs =10 | Ncs= 12 | Ncs =16 |
| 2 | 268 | 369 | 473 |
| 4 | 652 | 855 | 1009 |
| 6 | 1203 | 1542 | 1747 |

3.2 Lipophilic contributions to free energy of solubilization.

In this section, we discuss the independent free energy contributions identified in Equation 3. To illustrate these contributions, it is convenient to consider the model's simulation of the solubilization of n-octane ($N_{CO}=8$) in a micelle conformed by dodecyl tails ($N_{CS}=12$) and headgroup area (A_s) of 50 \AA^2 at $25 \text{ }^\circ\text{C}$. The result from this simulation is shown in Figure 8. Negative values in Figure 8 correspond to favourable thermodynamic contributions to solubilization (spontaneous reversible work). Positive contributions can be interpreted as free energy (reversible work) cost associated with the process of

solubilization. As illustrated in Figure 8, there are three favorable contributions, the net surfactant-surfactant interaction $W_{SS}(Ro)$, the surfactant-oil interaction $W_{SO}(Ro)$, and the tail domain mixing free energy $\Delta G_O^{Mix}(Ro)$. $W_{SS}(Ro)$ is the largest favorable contribution to the total free energy $W_T(Ro)$ of solubilization. In fact, $W_{SS}(Ro)$ can be considered as the primary lipophilic driver for micellar solubilization. According to VDW-FEM, the reason why $W_{SS}(Ro)$ is relatively large and negative at small micelle core radius is because in the swollen micelle the surfactant gains additional surfactant-oil interactions with the oil solubilized in the tail domain.

The surfactant-oil $W_{SO}(Ro)$ interaction provides the next largest favoring contribution to solubilization. However, as it becomes clear in the insert of Figure 8, this surfactant-oil contribution $W_{SO}(Ro)$ is counterbalanced by the oil-oil interaction $W_{OO}(Ro)$, which is understandable given that the core oil is extracted from an alkane environment and placed in an alkane environment. The mixing free energy in the tail domain, $\Delta G_O^{Mix}(Ro)$ is the smallest favorable contribution to solubilization. There are two contributions that oppose the solubilization of oils in micelles, the oil-oil interaction $W_{OO}(Ro)$ that compensates for the surfactant-oil interaction in the swollen micelle, and the free energy required to extract oil molecules from the oil phase to be solubilized in the tail domain, $W_{OT}(Ro)$. $W_{OT}(Ro)$ is the largest lipophilic interaction at large core radius (insert of Figure 8), and is also the main differentiator when comparing the solubilization of different alkanes, as discussed in the next section.

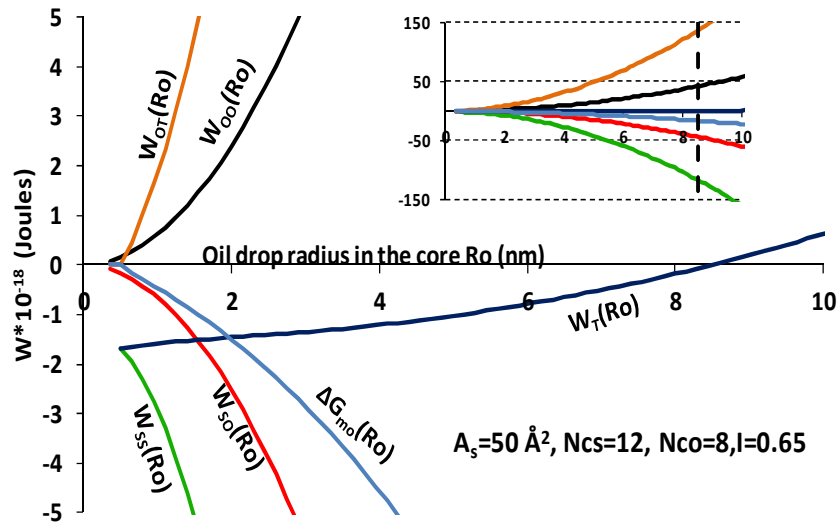


Figure 8. Lipophilic free energy contributions to the total free energy $W_T(R_o)$ for the solubilization of n-octane in C_{12} micelle ($A_s = 50 \text{ \AA}^2$) at $25 \text{ }^\circ\text{C}$ as a function of the micelle core radius. See section 3 for complete definitions of $W_{OO}(R_o)$, $W_{OT}(R_o)$, $W_{SO}(R_o)$, $W_{SS}(R_o)$ and $\Delta G_0^{Mix}(R_o)$.

3.3 Effect of molecular structure of oils and surfactants on solubilization

Figure 9 shows the total lipophilic free energy $W_T(R_o)$ of solubilizing different n-alkanes in a C_{12} micelle, same conditions of Figure 8, as a function of the micelle core radius (R_o). It can be observed that all the $W_T(R_o)$ curves exhibit parabolic shapes starting from a common negative value. This behavior indicates, except for hexane, the existence of an equilibrium condition in which oil swollen micelles have been formed. The behavior of these solubilization free energy curves observed is similar to other free energy curves proposed for microemulsion formation by other authors.^{6,51}

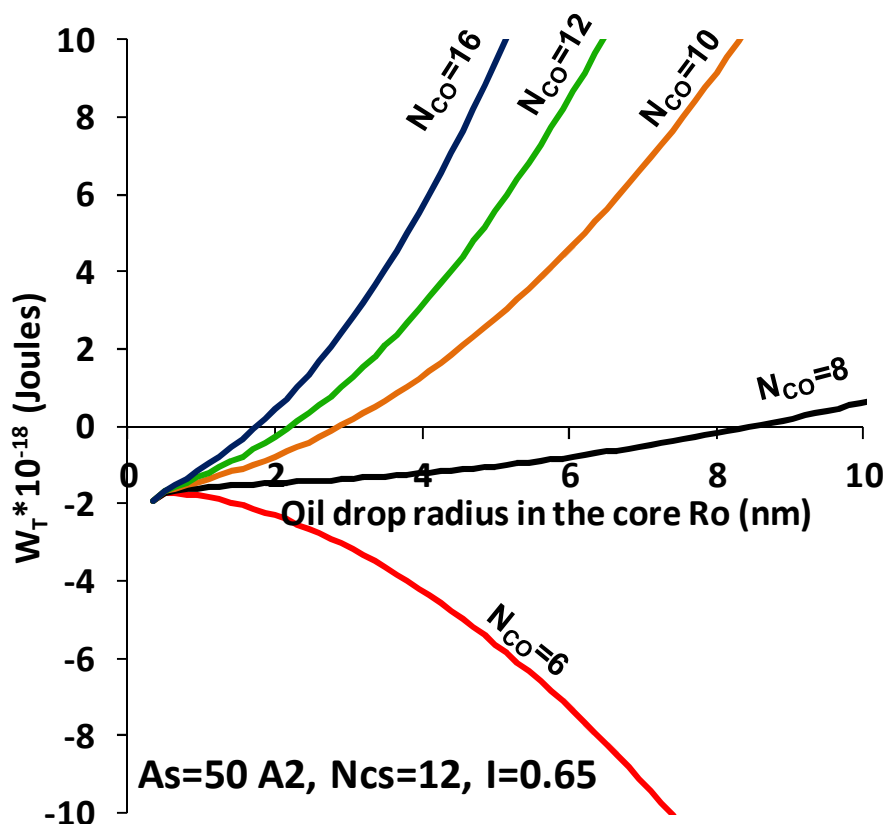


Figure 9. Free energy of oil solubilization of hexane ($N_{co}=6$), octane ($N_{co}=8$), decane ($N_{co}=10$), dodecane ($N_{co}=12$) and hexadecane ($N_{co}=16$) in micelles conformed by dodecyl surfactant tails ($N_{cs}=12$) and headgroup areas (A_s) of 50 \AA^2 as a function of the oil drop solubilized in the core at $25 \text{ }^\circ\text{C}$.

The reason for the existence of a common starting point is that this starting point is only dominated by the structure of the surfactant, which influences the $W_{SS}(R_o)$ interaction. The explanation for all the curves presenting a parabolic shape is that the volume of oil solubilized in the tail domain, which influences $W_{OT}(R_o)$, is proportional to the volume of the tail domain, which scales with the area of the core ($4\pi R_o^2$). The difference among the curves for different oils is due to their difference in cohesive energy (U), which directly influence the value of $W_{OT}(R_o)$. Larger alkanes have larger cohesive energies, which make them more energetically expensive to extract them from their oil phase to be solubilized in the tail domain of micelles, resulting in lower oil solubilization capacities. For the case of hexane in Figure 9, its cohesive energy is small enough that the $W_{SS}(R_o)$ interaction, which also accounts for the surfactant-oil interaction in the tail domain, overcomes $W_{OT}(R_o)$ leading to negative values of $W_T(R_o)$. In other words, hexane interactions with C_{12} tails and other hexane molecules in the tail domain are stronger

than the hexane-hexane interactions in the continuous oil phase. In fact, all the curves of Figure 9 can be turned completely negative if the fraction of the cohesive energy is reduced from $f=0.65$. The particular case of the solubilization free energy curve of hexane can be interpreted as if it would have established a bicontinuous or water in oil system.

Figure 10, similarly to Figure 9, presents the total lipophilic free energy $W_T(R_o)$ of solubilizing different n-alkanes, but in this case for a C_{10} micelle, as a function of the micelle core radius (R_o). The trends observed in Figure 10 are similar to those in Figure 9, but there are three differences worth discussing. The first one is that the value of $W_T(R_o)$ at the origin of the curves for C_{10} micelles is close to $-1E-18$ J, where as for C_{12} micelles in Figure 9 that value was closer to $-2E-18$ J. Another difference is that for hexane in Figure 10, $W_T(R_o)$ has an upward trend. This is due to the fact that the interaction hexane- C_{10} in the tail domain is not as strong as the interaction hexane- C_{12} , and it can't overcome the $W_{OT}(R_o)$ term. The third difference is that the solubilization curves for all the alkanes in C_{10} micelles produce more positive values of $W_T(R_o)$, at a given R_o , than the curves of Figure 9. Once again, this VDW-FEM prediction comes from the fact that W_{ss} interactions are weaker in C_{10} tail domains than in C_{12} domains.

The predicted effects of the size of the surfactant tail on oil solubilization are consistent with experimental trends reported in the literature.² The simulations presented in Figures 9 and 10 show also that the solubilization of alkanes increases with a decrease in the number of carbons, in agreement with experimental observations.^{1,26} The apparent big solubilization difference between hexane and any other alkane used in these simulations reflect trends observed in experimental studies.^{26,28}

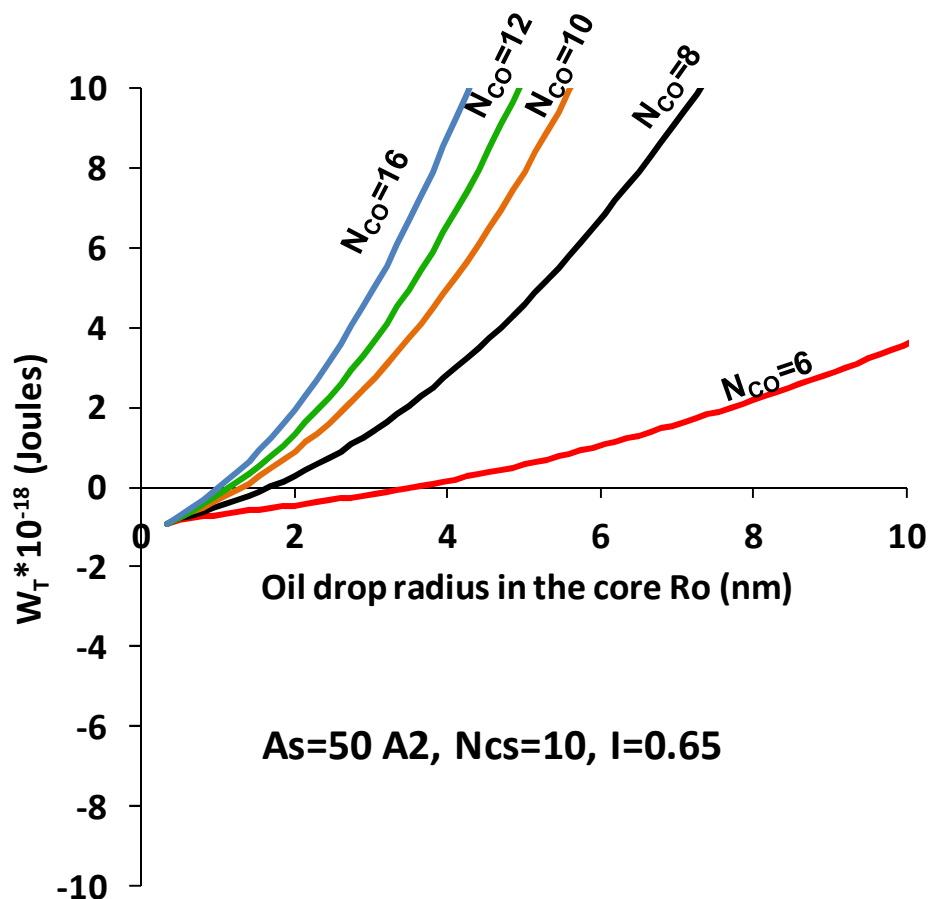


Figure 10. Free energy of oil solubilization of hexane ($N_{co}=6$), octane ($N_{co}=8$), decane ($N_{co}=10$), dodecane ($N_{co}=12$) and hexadecane ($N_{co}=16$) in micelles conformed by decyl surfactant tails ($N_{cs}=10$) and headgroup areas (A_s) of 50 A^2 as a function of the oil drop solubilized in the core at $25 \text{ }^\circ\text{C}$.

There are no systematic studies defining the surfactant headgroup areas established when the micelles become swollen or either studies involving the effect of the type of oil solubilized on the surfactant head group area. However, it has been consistently reported that for nonionic alkyl ethoxylated surfactants the planar air/water headgroup area generally increases when increasing the head group size.¹ Experimental studies also indicate that for the same alkyl ethoxylated surfactant tail, increases of headgroup size cause decrease in the amount of nonpolar oil solubilized in type I microemulsions.²⁶ Assuming that the planar air/water interface established by these surfactants is similar to the areas established by the same surfactants when conforming swollen micelles, one could conclude that

increases of headgroup area cause decrease in the solubilization of nonpolar oils. In agreement with the analysis here, other authors indicate that the solubilization of aliphatic hydrocarbons increase as the length of the of alkyl ethoxylated surfactant chain decreases.^{1,52}

If the curves for $W_T(R_o)$ in Figures 8-10 would have included hydrophilic interactions, then the core radius at which the total free energy (reversible work) of solubilization is zero would have corresponded to the equilibrium core solubilization radius. The $W_T(R_o)$ curve in Figure 8 shows an apparent equilibrium solubilization (~ 8 to 9 nm) because the maximum value of $I=0.65$ was used. A follow up study of this work will integrate hydrophilic and lipophilic interactions that could be compared with real equilibrium solubilization radii. However, the trends in apparent solubilization radii of Figures 9 and 10 can be used to describe the effect of lipophilic interactions on micellar solubilization. For example, the effect of surfactant headgroup area on the solubilization of alkanes is presented in Figure 11. Simulations considering hypothetical micelles made of C_{12} surfactants with head group areas of 40 , 50 , and 60 \AA^2 show that surfactants with smaller headgroup areas present higher apparent equivalent radius of total oil solubilized (R_e) at equilibrium for alkane smaller than decane. For larger alkanes, there are only small differences in solubilization. Other simulations that consider even smaller headgroup areas, around 35 or 30 \AA^2 , place the origin of the free energy curves of Figure 9 or 10 in the positive domain of the free energy. In this case, there is very little solubilization of oil in the tail domain, which, according to the model is the driving force for the overall solubilization in micelles. This theoretical calculation supports the experimental evidence that show that incorporating lipophilic additives (lipophilic linkers) that can segregate near the surfactant tails, extending the tail domain, can increase the solubilization capacity in micelles.^{53,24}

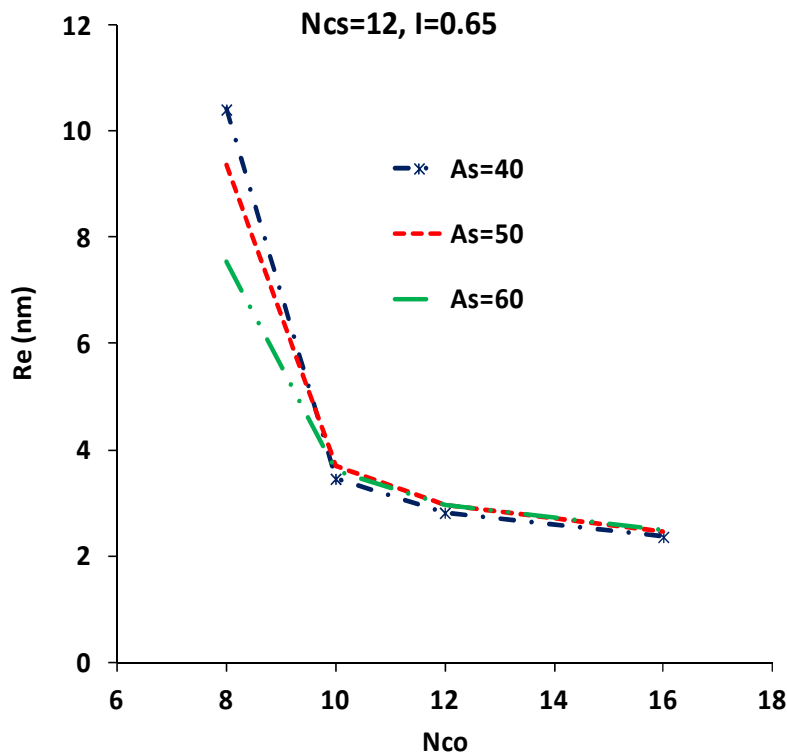


Figure 11: Equivalent radius of oil solubilization in micelles conformed by C_{12} surfactant as a function of solubilized alkane number (N_{co}), considering different headgroup areas (A_s) at 25 °C.

3.4 VDW-FEM and its relation to HLD-NAC

The HLD-NAC has been previously associated to the properties of microemulsion components, including empirical terms (K , N_{CO}) that seem to originate from the interplay of lipophilic interactions.^{23,54} In principle, the VDW-FEM framework should be able to predict the empirical terms in the HLD-NAC that result from lipophilic interactions. To test this hypothesis, we should acknowledge that, according to Equation C5 of the appendix, the net curvature interpretation of HLD provides reasonable estimations of oil solubilization radius.⁵⁵ Furthermore, if we consider hypothetical experiments carried out with various alkanes (N_{CO}) at reference temperature and salinity and with no cosurfactant, then, the terms $\varphi(A)$, $b(s)$ and $C_T * \Delta T$ vanish in Equation C2 so that:

$$\Delta(\text{HLD}) = -K * \Delta(N_{CO}) \quad (21)$$

Since we are considering oil in water microemulsions, the term $1/R_w$ in Equation C5, is disregarded. Additionally, knowing that the length scale parameter in the same equation is constant for a specific surfactant, the variation of the HLD with respect to R_o can be expressed as follow.

$$\frac{-\Delta(\text{HLD})}{2L} = \Delta\left(\frac{1}{R_o}\right) \quad (22)$$

Combining equations 21 and 22, a final expression is obtained as follow:

$$K * \Delta(N_{co}) = \Delta\left(\frac{2L}{R_o}\right) \quad (23)$$

Equation 23 derived from the HLD-NAC indicate that plots of $\Delta\left(\frac{2L}{R_o}\right)$ versus $\Delta(N_{co})$ should provide straight lines with slopes corresponding to K . This term in the HLD-NAC has been reported to vary from values of 0.1 to 0.2 for different combinations of surfactants and oils.^{23,56} To test the VDW-FEM, Equation 23 can be evaluated using predicted information of the VDW-FEM by obtaining the solubilization of different alkanes at their maximum solubilization capacity, which are extracted in part from Figures 9 and 10 at zero total free energy. Such evaluation can be made considering that the surfactant tail length L_s in the VDW-FEM correlates with the length scale parameter L in the HLD-NAC.

Figure 12 illustrates the variation of solubility of different alkanes in terms of $\left(\frac{2L}{R_o}\right)$ versus N_{co} for two different straight-chain surfactant tails at 25 °C. In both cases, the micelles were assumed to have headgroup areas of 50 \AA^2 and that the lipophilic energy cost to solubilize these oils in between surfactant tails was 65% of the cohesive energy of the oil. The upper and lower curves, corresponding to C_{10} and C_{12} surfactants, show that they can be approximated to straight lines in agreement with the hypothesis (Equation 23). The magnitude of the slopes, in both cases, is within the range of K values reported in the literature.^{23,56} The slight curvature observed in both curves has also been observed by other researchers.⁵⁷ An upcoming article that integrated the hydrophilic interactions show that the trends reflected in Figure 12 are maintained, even when the fraction of the cohesive energy, I , is reduced to values as low as 0.45

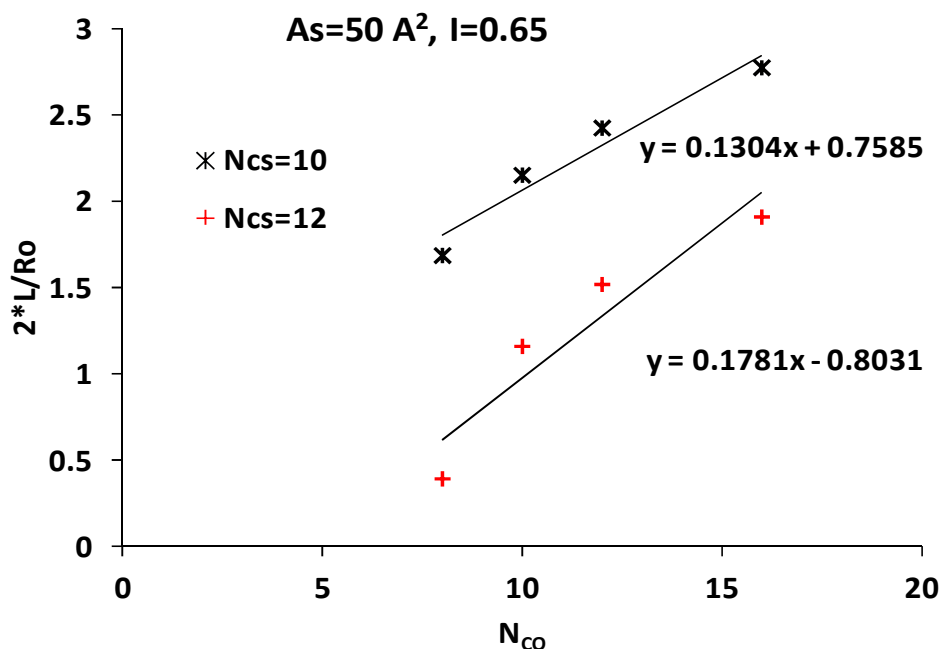


Figure 12. $2L/R_o$ versus the alkane carbon number (N_{co}) considering decyl ($N_{cs}=10$) and dodecyl ($N_{cs}=12$) surfactant tails considering for both cases headgroup areas (A_s) of 50 \AA^2 at 25°C .

4. Conclusions

A thermodynamic framework to estimate the magnitude of the lipophilic free energy contributions to oil solubilization in micelles was introduced. The free energy contributions are calculated considering a process of solubilization where oil is extracted from a continuous oil phase and surfactants are extracted from empty micelles to form oil-swollen micelles. This VDW-FEM approach describes well the solubilization features of n-alkanes in micelles considering changes of surfactant tail length, type of alkane and headgroup area. At this point, the VDW-FEM framework does not contain any adjustable parameter. Curves of total lipophilic free energy contributions as a function of micelle core radius reveal that the solubilization of oil in the tail domain of oil-swollen micelles is a key factor in driving the solubilization of oils. The main differentiator in the solubilization capacities of different oils is their respective cohesive energy. Oils with larger cohesive energies are difficult to solubilize, while surfactants with longer tails produce larger solubilizations. While all these trends have been known for a long time, the VDW-FEM framework introduces a quantitative method to predict these trends. The trends identified

through the VDW-FEM were compared to trends predicted by the semi-empirical HLD-NAC model. The term $K \cdot N_{CO}$ of the HLD was confirmed theoretically, as well as the experimental value of K . Lastly, the free energy model is simple and does not require any special consideration requiring large computer capacity, making it more approachable compared to other molecular simulation methods.

While there is agreement between the VDW-FEM predicted trends and the experimental trends, there could be additional interactions or terms that might be needed to be considered in the future. For example, solvation effects, preferential oil solubilization when solubilizing oil mixtures, and others. The relatively simple framework of the VDW-FEM could be further modified in the future to include these and other effects.

AUTHOR INFORMATION

Corresponding Author

*Tel: 416-946-0742. Fax: 416-978-8605. E-mail: acosta@chem-eng.utoronto.ca

Note: The authors declare no competing financial interest

APPENDIX

Appendix A: Aggregation aspects of empty and swollen micelles

To account for the lipophilic interactions as well as to define variables associated to the mathematical representation of empty and swollen micelles, there is need to estimate the surfactant aggregation number during a solubilization process of oil in micelles. The surfactant aggregation number N_{em} of an empty micelle is calculated considering the close packed configuration of surfactant tails, as given by the following equation:

$$N_{em} = \frac{4\pi[(0.8L_s + d_o)^3 - d_o^3]}{3V_{ms}} \quad (A1)$$

Where L_s is the surfactant tail length and d_o is the radius of an empty volume at the center of the sphere, which is 20% the surfactant tail length as shown in Figure A1. V_{ms} is the molecular volume of the alkane representing a surfactant tail.

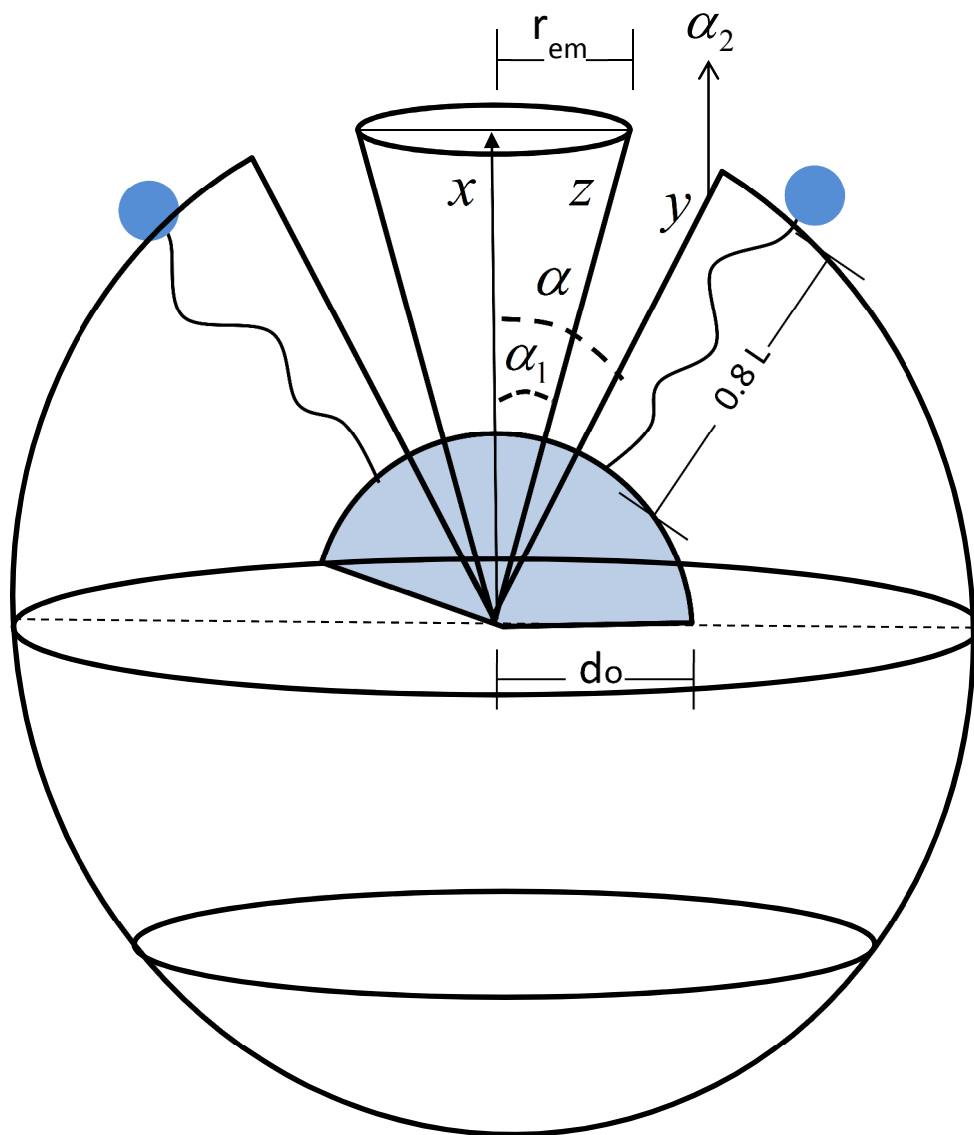


Figure A1: Adapted from reference **Error! Bookmark not defined.** to describe the terms of Equation 14.

The surfactant aggregation number in swollen micelles $N_{AR}(Ro)$ can be defined by:

$$N_{AR}(Ro) = \frac{4\pi(Ro + \delta + L_S)^2}{A_S} \quad (A2)$$

Where Ro is the oil drop radius solubilized in the core and A_S is the surfactant headgroup area, which is an input parameter obtained experimentally using the Gibbs adsorption equation and reported in the

literature.¹ The surfactant head group area has been recognized to be located at the neck of the surfactant at the point in which the headgroup and the tail meet.⁴⁸

In addition to the surfactant aggregation number $N_{AR}(Ro)$, we also use the concept of lipophilic aggregation number $N_{AT}(Ro)$. The lipophilic aggregation number $N_{AT}(Ro)$ reflects the number of lipophilic entities (surfactant tails and oil solubilized in between tails) present in the surfactant tail domain and it is calculated assuming that the tail domain is occupied by oil molecules similar to the surfactant tails as follow:

$$N_{AT}(Ro) = \frac{4\pi[(Ro + \delta + L_S)^3 - (Ro + \delta)^3]}{3V_{ms}} \quad (A3)$$

It is worthwhile to mention that at the beginning of the solubilization, the surfactant aggregation number is controlled by the close-packed configuration of the tails as calculated with Equation A3. Once the minimum neck area A_S is reached, the aggregation number is determined by Equation A2. This condition to estimate the surfactant aggregation number holds in a very narrow range of values almost irrelevant to the model. However, the lipophilic aggregation number is a useful assumption applied to account for the surfactant interactions and to omit the discrete character of the tail domain to enable the calculation of the Hamaker constant using the Lifshitz continuum approach. This fact also allows to reflect the synergistic aspect of the oil in between tails contributing to the surfactant interactions, as discussed in sections 4.2 and 4.3. Relevant to the molecular interactions is the number of oil molecules solubilized in between surfactant tails $N_{OS}(Ro)$, which is estimated by:

$$N_{OS}(Ro) = \frac{V_{sh}(Ro) - N_{AR}(Ro) * V_{ms}}{V_{mo}} \quad (A4)$$

Where V_{mo} is the molecular volume of the oil solubilized in between tails. The surfactant tails establish a spherical shell volume $V_{sh}(Ro)$ proportional to the surfactant tail length, which is calculated using the following equation:

$$V_{sh}(Ro) = \frac{4}{3}\pi[(Ro + \delta + L_s)^3 - (Ro + \delta)^3] \quad (A5)$$

Appendix B: Geometric aspects of the mathematical representation of empty and swollen micelles

EMPTY MICELLES

To define the variables and boundary conditions of integral 14, it is necessary to refer to Figure A1. Thus, α_2 is an integration boundary that defines the coneless shell, which is defined by the following equation in accordance to Figure A1:

$$\alpha_2 = \alpha_1 + f\alpha_1 \quad (B1)$$

The coefficient f establishes the separation distance between the cone and the shell and has been determined to be equal to 0.58.³³ α_1 is the angle that defines the radius of the truncated cone, which represents a surfactant tail of an empty micelle, as graphically depicted in Figure 4B. Its calculation proceeds as:

$$\alpha_1 = \text{atan}\left(\frac{r_{em}}{0.8L_s + d_o}\right) \quad (B2)$$

r_{em} is the external radius of the cone representing a surfactant tail of an empty micelle, as:

$$r_{em} = \sqrt{\frac{A_{em}}{\pi}} \quad (B3)$$

For empty micelles, the area of the surfactant is given by the close-packed tails and it is obtained from:

$$A_{em} = \frac{4\pi(0.8L_s + d_o)^2}{N_{em}} \quad (B4)$$

When the micelle is empty, the area A_{em} is defined by the close packed configuration of the tails. Once the micelle starts solubilizing oil in its core and tail domain, this area reaches the value of A_s and remains constant during the solubilization process.

SWOLLEN MICELLES

Defining the terms needed to solve the integral 15 follows an analogous procedure to the one made to define the terms to solve Equation 14. Consequently, the description of the angle that defines the integration limit of the coneless shell, in analogy to Equation 14 is now defined as a function of the oil solubilized in the core, as:

$$\alpha_{2s}(Ro) = \alpha_{ms}(Ro) + f\alpha_{ms}(Ro) \quad (B5)$$

So that the angle that describe the cone is now:

$$\alpha_{ms}(Ro) = \text{atan}\left(\frac{r_m(Ro)}{R_o + \delta + L_s}\right) \quad (B6)$$

The radius of the cone established by the tail is obtained from:

$$r_m(Ro) = \sqrt{\frac{A_s(Ro)}{\pi}} \quad (B7)$$

Considering as reference Figure A1, and in analogy to the estimation of the cone area of empty micelles in Equation B4, the area established by the surfactant tails and oil solubilized in between the tails is given by:

$$A_s(Ro) = \frac{4\pi(R_o + \delta + L_s)^2}{N_{AT}(Ro)} \quad (B8)$$

Appendix C: The HLD-NAC equations

The HLD equations for ionic (Equation C1) and for nonionic (Equation C2) surfactants are as follow:⁵⁸

$$HLD = \ln(S) - K * N_{CO} - f(A) + C_c - a_T * \Delta T \quad (C1)$$

$$HLD = b(s) - K * N_{CO} - \varphi(A) + C_T * \Delta T + C_{cn} \quad (C2)$$

where S represents the electrolyte concentration, N_{CO} is the equivalent alkane carbon number (EACN) of the oil phase. $f(A)$ and $\varphi(A)$ are functions related to the type of co-surfactant and its concentration. ΔT is a temperature deviation from 25°C. K, b, a_T and c_T are empirical constants which vary depending on the electrolyte and surfactant used. In order to define the nature and behavior of surfactants at comparable states within the HLD concept, the following reference conditions have been established: $T_{ref} = 25$ °C, $N_{CO}=0$ (Benzene), $f(A) = \varphi(A) = 0$, and $S_{ref} = 1 \text{ g NaCl} / 100 \text{ ml}$ for ionic surfactants while $S_{ref} = 0$ (NaCl) for nonionic surfactants.^{23,58} C_c and C_{cn} stand for the characteristic curvature of ionic and nonionic surfactants, respectively. The characteristic curvature of an ethoxylated nonionic surfactant is:²³

$$C_{cn} = \alpha_s - N_{ES} \quad (C3)$$

where N_{ES} is the number of ethylene oxide groups in the surfactant and α_s is a parameter that for linear alkyl ethoxylate surfactants depends on the number of carbons (N_{CS}) in the alkyl group of the tail:²³

$$\alpha_s = 0.28 * N_{CS} + 2.4 \quad (C4)$$

The HLD was combined with the concept of curvature and the critical scaling theory, work that led to the HLD-NAC model, and the realization that the HLD reflects the curvature of the surfactant at the oil-water interface.^{23,54,58} The NAC equations are:⁵⁴

$$H'_n = \frac{H_n}{2} = \frac{1}{2} \left(\frac{1}{R_o} - \frac{1}{R_w} \right) = \frac{-HLD}{2L} \cong \frac{1}{R'} \quad (C5)$$

$$H_a = \frac{1}{2} \left(\frac{1}{R_o} + \frac{1}{R_w} \right) \leq \frac{1}{\xi} \quad (C6)$$

H'_n is a net curvature term that connects the HLD with the area-averaged curvature of the microemulsion drops, as reported elsewhere.**Error! Bookmark not defined.** R' is a term that describes the radius of curvature at the water-oil interface. H_a , the average curvature, describes the surface area to volume ratio of the dispersed phase. R_o and R_w are the radii of coexisting hypothetical droplets of oil and water. L is a length parameter that scales with the extended length of the surfactant tail, and ξ is the characteristic length of the microemulsion, which represents the maximum solubilization capacity.⁵⁸

NOMECLATURE

LIST OF ACRONYMS AND SIMBOLS

A_{CO} : surfactant-oil interactions in Winsor's R ratio equation

A_{em} : headgroup area of an empty micelle

A_{CW} : surfactant-water interactions in Winsor's R ratio equation

A_{HH} : surfactant-Surfactant interactions in the aqueous phase in Winsor's R ratio equation

A_{LL} : surfactant-Surfactant interactions in the oil phase in Winsor's R ratio equation

A_{ls-i} : Lifshitz- based Hamaker constant used to calculate oil-oil or surfactant-surfactant interactions
 A_{ls} : Lifshitz-based Hamaker constant used to calculate the surfactant-oil interactions
 A_{OO} : oil-oil interactions in the Winsor's R_w ratio equation
 A_{oo} : Liftshitz-based oil-oil Hamaker
 A_s : headgroup area obtained from the Gibbs adsorption equation
 A_{so} : surfactant-oil Hamaker constant
 A_{ss} : surfactant- surfactant Hamaker constant
 $A_s(RO)$: close packed surfactant/oil area established at the oil- water interface in a swollen micelle
 A_{WW} : water-water interactions in Winsor's R ratio equation
 a : parameter that provides temperature dependence to the dielectric constant
 a_T : empirical constant in the HLD equation
 b : parameter that provides temperature dependence to the dielectric constant
 $b(S)$: electrolyte concentration in the HLD equation for nonionic surfactants
 c : parameter that provides temperature dependence to the dielectric constant
 C : van der Waals dispersion coefficient
 C_c : characteristic curvature of ionic surfactants
 C_{cn} : characteristic curvature of nonionic surfactants
 C_T : empirical constant in the HLD equation
 d : parameter that provides temperature dependence to the dielectric constant
 d_o : radius of an empty whole of an empty micelle
 dV_i : volume element of a body
 f : constant that defines the separation distance between a cone and a shell
 $f(A)$: function related to the cosurfactant used with ionic surfactants
 HLD : Hydrophilic-lipophilic Difference
 H_a : average curvature in the HLD model
 H_n : net curvature in the HLD equation
 H'_n : revised net curvature in the NAC equations.
 h : Planck's constant
 I : energy needed to transport oil from its liquid phase to the surfactant tail domain expressed as a fraction of its cohesive energy.
 $I(RO)$: energy needed to transport oil from its liquid phase to the surfactant tail domain expressed as a fraction of its cohesive energy estimated as a function of its solubilization in the core of a micelle.
 I_A : first Ionization Potential of molecule A
 I_B : first Ionization Potential of molecule B
 K : empirical constant in the HLD equation
 L : length scale parameter in the HLD-NAC equation
 L_s : length of the surfactant

$\ln(S)$: electrolyte concentration in the HLD equation for ionic surfactants

N_{CO} : equivalent alkane carbon number in the HLD equation

N_{ES} : number of ethylene oxide groups of a surfactant

$N_{OC}(Ro)$: number of oil molecules solubilized in the core of a microemulsion

$N_{OS}(Ro)$: number of oil molecules solubilized in the tail domain of a micelle

N : Avogadro's number

$N_{AR}(Ro)$: surfactant aggregation number in a swollen micelle

$N_{AT}(Ro)$: lipophilic aggregation number or number of lipophilic entities within the tail domain of a micelle

N_{em} : surfactant aggregation number in an empty micelle

R : universal gas constant

R' : corrected radius of oil or water providing better estimate of the curvature at the water-oil interface

R_w : Winsor's R ratio

R_O : radius of the oil solubilized in the core or hypothetical radii of water in the NAC equation

R_W : hypothetical water radii in the NAC equation

$R_e(Ro)$: equivalent radius of total oil solubilized in a micelle as function of the oil drop size in the core

r : separation distance between two molecules

r_{em} : radius of an empty micelle

$r_m(Ro)$: radius of a truncated cone established by surfactant tails and oil in the tail domain of a micelle

S : salinity at any other condition different from optimum

s : salinity at optimum formulation conditions in the HLD equation

S_{ref} : reference salinity conditions for nonionic or ionic surfactants

T : temperature

U : cohesive energy

$V_{sh}(Ro)$: shell volume of the surfactant tail domain L_s

V_{mo} : molecular volume of oil

V_{ms} : molecular volume of the alkane representing a surfactant tail

VDW: van der Waals

$V_{OC}(Ro)$: volume of oil solubilized in the core of a microemulsion

$V_{OS}(Ro)$: volume of oil solubilized in between tails

$W_{bs}(Ro)$: interaction energy of a sphere containing all the oil solubilized in a micelle with a shell

$W_{OO}(Ro)$: energy cost to extract oil from its continuum to be solubilized in the core of a micelle

$W_{OT}(Ro)$: energy cost to extract oil from its continuum to be solubilized in the tail domain of a micelle

W_{PS} : surfactant-surfactant interactions in an empty micelle

$W_{PSO}(Ro)$: surfactant-surfactant interactions in a swollen micelle

$W(r)$: term to define the general expression to calculate the interaction of two bodies

$W_{SO}(Ro)$: surfactant-oil interaction

$W_{SS}(Ro)$: free energy change of surfactants during a solubilization process.

$W_T(Ro)$: total free energy of oil solubilization in micelles

$W_{cone-shell}(Ro)$: interaction of a cone with a shell

x : variable used to define the volume element of a ring and the volume element of a truncated cone

$x_o(Ro)$: fraction of oil molecules in a mixture of tails and oils in the tail domain of a micelle

$x_s(Ro)$: fraction of surfactant tails in a mixture of tails and oils in the tail domain of a micelle

y : variable used to define the volume element of a cone-less shell

GREEK LETTERS

α : variable in spherical coordinates used to define the volume element of a coneless shell

α_s : parameter that represents the molecular structure of the surfactant

α_1 : angle that defines the radius of a cone in an empty micelle

α_2 : initial limit of integration of the cone-less shell in an empty micelle

$\alpha_{ms}(Ro)$: Angle that defines the radius of a cone in a swollen micelle

$\alpha_{2s}(Ro)$: Initial limit of integration of the cone-less shell in a swollen micelle

α_{PA} : molecular polarizability of molecule A

α_{PB} : molecular polarizability of molecule B

δ : interfacial separation distance define to be 0.165 nm

ΔT : temperature difference from the reference conditions in the HLD equation

ΔS_{mo}^{Mix} : entropy of mixing oil in between surfactant tails of an empty micelle

ΔH_{mo}^{Mix} : enthalpy of mixing oil in between surfactant tails of an empty micelle

$\Delta G_{mo}^{Mix}(Ro)$: free energy of mixing oils with surfactant tails

ε : dielectric constant

$\varepsilon_i(T)$: dielectric constant of liquids as a function of temperature

ε_0 : vacuum permittivity

n_i : refractive index

$\varphi(A)$: function related to the cosurfactant used with nonionic surfactants

ρ_i : molecular density of an interacting body

ν_e : characteristic absorption frequency

κ : Boltzmann constant

Ω : shell layer that represents the extent of the oil shell

ξ : variable used to define a volume element of a spherical shell

REFERENCES

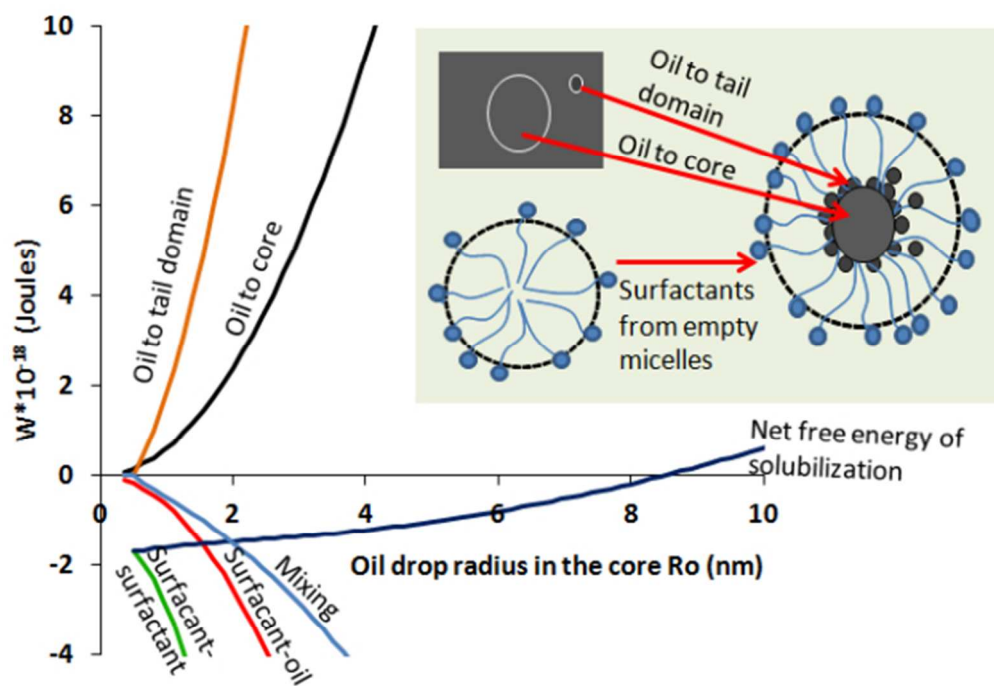
1. M. J. Rosen, Surfactants and Interfacial Phenomena, 3rd. Ed., John Wiley & Sons, New York, 2004.

2. K. Holmberg, B. Jonsson, B. Kronberg, and B. Lindman, *Surfactants and Polymers in Aqueous Solution*, 2nd. Ed., John Wiley and Sons, England, 2003.
3. D. Myers, *Surfaces, Interfaces and Colloids; Principles and Applications*. 2nd Ed. John Wiley & Sons, USA, 1999.
4. J. L. Salager, *Prog. Colloid Polym. Sci.*, 1996, 100, 137-142.
5. A. Ben-Naim, *Molecular Theory of Water and Aqueous Solutions*, Part II, World Science, USA, 2011.
6. B. Lemaire, P. Bothorel and D. Roux, *J. Phys. Chem.*, 1983, Vol. 87, No. 6.
7. N. Naouli, H. L. Rosano and M. Kanouni, *J. Dispersion Sci. Technol.*, 2011, 32, 359-364.
8. J. Jouffroy, P. Levinson and P. G de Gennes, *J. Phys.*, 1982, 43, 1241-1248
9. J. N. Israelachvili and D. J. Mitchell, B. W. Ninham, *J. Chem. Soc., Faraday Trans. 2*, 1976, 72, 1525-1568
10. D. J. Mitchell and B. W. Ninham, *Micelles*, *J. Chem. Soc. Faraday Trans. 2*, 1981, 77, 601-629.
11. M. Grimson, and F. Honary, *Phys Lett.*, 1984, Vol. 102A, Number 5, 6.
12. S. A. Safran, and L. A. Turkevich, *Phys. Rev. Lett.*, 1983, 50, 24
13. R. Nagarajan and E. Ruckenstein, *Langmuir*, 2000, 16, 6400-6415.
14. J. C. Shelley, and M. Y. Shelley, *Current Opinion in Colloid & Interface Science*, 2000, 5, 101-110.
15. T. Kurokawa, N. Urakami, K. Nakaya, A. Sakashita, M. Imai and T. Yamamoto, *Soft Matter*, 2011, 7, 7504-7510.
16. R. G. Larson, L. E. Scriven and H. T. Davis, *J. Chem. Phys.* 1985, 83, 2411.
17. R. G. Larson, *J. Chem. Phys.* 1988, 89, 1642
18. B-A, Rezan, A. K. Mohammad, N. Mehdi., *J. Chin. Chem. Soc.*, 2008, 55, 716-723.
19. B. W. Ninham and P. Lo Nostro, *Molecular Forces and Self Assembly in Colloid Nano Sciences and Biology*. Cambridge University Press, Cambridge, USA, 2010
20. V. A. Parsegian, *van der Waals Forces. A Handbook for Biologists, Chemists, Engineers, and Physicists*. Cambridge University Press, Cambridge, USA, 2006.
21. S. Queste, J. L. Salager, R. Strey, and J. M. Aubry., *J. Colloid Interface Sci.* 2007, 312, 98-107.
22. F. Bouton, M. Durand, V. Nardello-Rataj, M. Serry, and J-M. Aubry, *Colloids Surf., A.*, 2009, 338, 142-147.
23. E. Acosta, *Colloids Surf. A*, 2008, 320, 193-204.
24. D. A. Sabatini, E. Acosta, J. H. H. Harwell, *Curr. Opin. Colloid Interface Sci.* 2003, 8, 316-326.
25. O. S. Dinesh, *Micelles Microemulsions and Monolayers Science and Technology*, Macel Dekker, New York, 1998
26. S. M. Diallo, L. M. Abriola and W. J. Weber, *Environ. Sci. Technol.*, 1994, 28, 1829-1837.
27. H. Høiland and A. M. Blokhus, *Handbook of colloid and Surface Chemistry*, (Birdi, K. D. Ed.), CRC Press, 3rd. Ed., USA, 2009.
28. M. Bourrel, R. S. Schechter, *Microemulsions and Related Systems: Formulation, Solvency, and Physical Properties*. Marcel Dekker Incorporated, USA, 1988.

29. P. Winsor, *Solvent Properties of Amphiphilic Compounds*, Butterworth, London, 1954
30. T. Crossgrove, *Colloid Science: Principles, Methods and Applications*, Blackwell Publishing Ltd, UK, 2005.
31. J. N Israelachvili, *Intermolecular and Surface Forces*, 2nd ed. Academic Press, New York, 1992.
32. C. Huh, *J. Colloid Interface Sci.*, 1979, 71, 2.
33. A. Boza and E. Acosta, *J. Phys. Chem. B*, 2012, 116, 14051-14061.
34. J. G. E. M. Fraaije, K. Tandon, S. Jain, J.-W. Handgraaf and M. Buijse, *Langmuir* 2013, 29, 2136-2151.
35. C. Browarzik, D. Browarzik, and J. Winkelmann, *J. Fluid Phase Equilib.* 2010, 296, 82-87.
36. Z. Qiu and J. Texter, *Curr Opin Colloid Interface Sci.*, 2008, 13, 252-262.
37. J. Eastoe, and D. C. Steytler, *Langmuir* 2006, 9832-9842
38. B. J. Carroll, *J. Colloid Interface Sci.*, 1981, 79, 1.
39. E. H. Yildirim, *Surface Chemistry of Solid and Liquid Interfaces*, Blackwell Publishing, USA, 2006.
40. V. A. Kirsch, *Adv. Colloid Interface Sci.*, 2003, 104, 311-324.
41. D. R. Lide, D.R. *Handbook of Chemistry and Physics*, 75th, ed; CRC Press: New York, 1995.
42. Z.-Y. Yu and R. W. Flumerfelt, *Ind. Eng. Chem. Res.*, 1996, 35, 3399-3402.
43. C. S. Dunaway, S. D. Christian and J. F. Scamerhon, *Solubilization in Surfactant Aggregates (Christian and Scamehorn Ed.)*. Marcel Dekker, Vol. 55, New York, 1995.
44. E.W. Lemmon, M.O. McLinden and D.G. Friend, "Thermophysical Properties of Fluid Systems" in *NIST Chemistry WebBook*, NIST Standard Reference Database Number 69, Eds. P.J. Linstrom and W.G. Mallard, National Institute of Standards and Technology, Gaithersburg MD, 20899, <http://webbook.nist.gov>, (retrieved June 25, 2013).
45. G. Maffiolo, J. Vidal and H. Renon, *Ind. Eng. Chem. Fundam.*, 1972, 11, 1.
46. S. Outcalt, A. Laesecke and T. J. Fortin, *J. Chem. Thermodyn.*, 2010, 42, 700–706.
47. R. Zana, *Surfactants Solutions; New Methods of Investigation (R. Zana, ed.)* Marcel Dekker, New York, 1987.
48. E. Acosta, E. Szekeres, J. Harwell, B. Grady and D. Sabatini, *Soft Matter*. 2009, 5, 551-561.
49. K. Yoshihara, H. Ohshima, N. Momozawa H. Sakai, and M. Abe, *Langmuir* 1995, 11, 2979-2984.
50. P. Lianos, J. Lang and R. Zana, *J. Phys. Chem.*, 1982, 86, 4809-4814.
51. E. Ruckenstein and J. C. Chi, *J. Chem. Soc., Faraday Trans. 2*, 1975, 71, 1690-1707.
52. S. Saito, *J. Colloid Interface Sci.*, 1967, 24, 227-234.
53. M. Miñana-Perez, A. Graciaa, J. Lachaise and J. L. Salager, *Colloids Surfaces A: Physicochem. Eng. Aspects*, 1995, 100, 217-224.
54. S. Kiran and E. Acosta, *J. Ind. Eng. Chem. Fundam*, 2010, 49, 3424-3432.
55. E. Acosta, E. Szekeres, D. A. Sabatini and J. H. Harwell, *Langmuir*, 2003, 19, 186-195.
56. A. Witthayapanyanon, J. H. Harwell, and D. A. Sabatini, *J. Colloid Interface Sci.*, 2008, 325, 259-266.

57. D. K. Rout, R. Goyal, A. Nagarajan, and P. Paul, in *Microemulsions- An Introduction to Properties and Applications* (R. Najjar Ed.), INTECH, Croatia, 2012.

58.E. Acosta, J. Yuan and S. Bhakta, *J. Surfactant Deterg.*, 2008, 11, 145-158.



Lipophilic contributions to the free energy of solubilization
53x39mm (300 x 300 DPI)